A Simple Cardiac Model Exhibiting Stationary Discordant Alternans

Tanawit Sae Sue
Supervisor: Professor David G. Schaeffer

Date: 2011-4-25

1 Introduction

The term *alternans* refers to a period-doubling bifurcation that occurs in rapidly-paced cardiac cells: although all stimuli are equally spaced, short and long action potentials alternate with one another. Cardiac waves that propagate in extended tissue often suffer phase reversals at various locations, a phenomenon that is known as *discordant alternans*. Even simulations cannot capture the full complexity of this phenomenon with realistic cardiac models in three-dimensional geometry. Significant insight into the phenomenon has been gained from the study of simple cardiac models propagating in just one dimension, and this is the context of the present paper.

The patterns of phase reversals may be either stationary or traveling. In the figure below, taken from reference [1], the former are illustrated in the upper figure, the latter, in the lower figure. Applying the weakly nonlinear analysis of Echebarria-Karma [2], Dai and Schaeffer [1] showed that which pattern actually occurs in a given simulation as the pacing rate is increased depends on a dimensionless combination of physiological parameters. In simulations with the simplest cardiac model, the two-current model of [4], only the case of traveling discordant alternans is ever observed. Stationary patterns have been observed, but only in simulations of physiologically complicated cardiac models. The goal of this paper is to study a simple cardiac model—the three-current model introduced by Fenton-Karma [3]—in which stationary discordant alternans may be observed in simulations. In the two-current model the dependence of the action potential duration (APD) on the diastolic interval (DI) is closely tied to the dependence of the wave speed (c) on DI, while in the three-current model separate parameters control the dependence of APD and c on DI. This flexibility allows us to choose parameters that locate the model in the regime of stationary discordant alternans. (These terms will be defined more carefully in the body of the paper.)

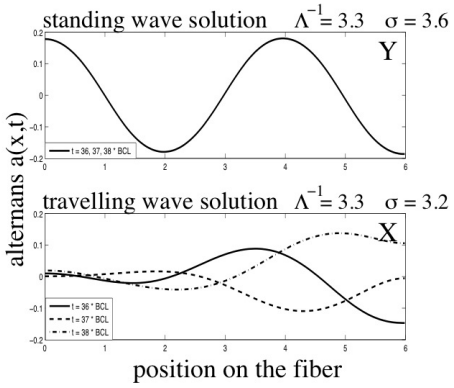

Figure 1: *Stationary and traveling discordant alternans.*

2 The Three-current Model for a Single Heart Cell

The three-current model in a single cell consists of three differential equations involving variables, which are the transmembrane voltage $v(t)$, the fast gate variable $f(t)$, and the slow gate variable $s(t)$ (variables are all dimensionless and scaled to range from 0 to 1). The system of differential equations is given as

$$\frac{dv}{dt} = J_{strong}(v,f) + J_{weak}(v,s) - J_{ung}(v), \quad ------(1)$$

$$\frac{df}{dt} = \begin{cases} \frac{-f}{\epsilon_{close}} & \text{, if } v > v_{crit}; \\ \frac{(1-f)}{\epsilon_{open}} & \text{, if } v < v_{crit}, \end{cases} \quad ------(2)$$

$$\frac{ds}{dt} = \begin{cases} \frac{-s}{\tau_{sclose}} & \text{, if } v_{thr} < v; \\ \frac{-s}{\tau_{fclose}} & \text{, if } v_{crit} < v < v_{thr}; \\ \frac{1-s}{\tau_{open}} & \text{, if } v < v_{crit}, \end{cases} \quad ------(3)$$

The strong inward current, weak inward current, and outward current, have the form

$$J_{strong} = \frac{f}{\tau_{strong}}(1-v)\chi(v-v_{crit}), \quad J_{weak} = \frac{s}{\tau_{weak}}\chi(v-v_{thr}), \quad J_{ung} = \frac{v}{\tau_{ung}},$$

where $\chi(x)$ denotes the indicator function of the set of non-negative numbers, i.e. $\chi_{[0,\infty)}(x)$. The typical values of parameters for the model are:

$\tau_{strong} = 1$ msec	$\tau_{sclose} = 500$ msec
$\tau_{weak} = 20$ msec	$\tau_{fclose} = 20$ msec
$\tau_{ung} = 20$ msec	$\tau_{open} = 50$ msec
$\epsilon_{close} = 10$ msec	$v_{crit} = 0.1$
$\epsilon_{open} = 10$ msec	$v_{thr} = 0.6$

In addition, the model includes a parameter v_{stim} whose default value is set up to be 0.4; the significance of this parameter will be discussed in next section. These parameters are adjustable, however in analyzing the model, we will assume that

$$\tau_{strong} \ll \tau_{weak} \approx \tau_{ung} \approx \tau_{fclose} \ll \tau_{sclose}.$$

2.1 Response to a Single Stimulus

Let us describe the response to a single stimulus, an event called an action potential. Assume that the system starts from the stable equilibrium of eq.(1,2,3) at $(v,f,s) = (0,1,1)$. An external stimulus is then applied causing the voltage to jump away from the equilibrium at 0 to v_{stim}, in a very short time. The external stimulus then disappears, leaving the heart cell to be driven by its own dynamics until it comes back to the equilibrium (or, in the case of multiple stimuli, until a new stimulus arrives). The voltage continues to rise even with no further contribution from the stimulus. There are three "forces" driving the voltage to rise and fall which can be categorized into two groups: inward (J_{strong} + J_{weak}) and outward (J_{ung}) currents. As the voltage increases, the gate variables begin to close permitting less and less inward current to flow in. On the contrary, the ungated current increases in the same direction as the voltage and independently of the gate variables. Once the outward current exceeds the inward current, the voltage will start dropping and continue doing so until it hits zero.

A response such as above is a typical response. It can be further divided into 3 phases as follows:

- 1. A rapid rise of the voltage due to domination of the strong current. The voltage increases very quickly relative to s, whose change is small throughout the phase. On the other hand, f decreases dramatically, especially toward the end of the phase ($v \to 1$), causing a significant fall in J_{strong}

- 2. The second phase begins when the voltage starts falling as the strong current is beginning to disappear and the system is instead governed by J_{weak} and the stronger J_{ung}. The voltage continues to fall even faster when v goes under v_{thr} because J_{weak} now vanishes leaving J_{ung} as the only active current. The fast gate stays small throughout the entire phase, while the slow gate is constantly closing. It is not until the end of the phase when $v = v_{crit}$ that both gates will begin to open.
- 3. The gates slowly reopen while the voltage stays small. The recovery of the gates continues until either the next stimulus arrives or the system comes back to equilibrium.

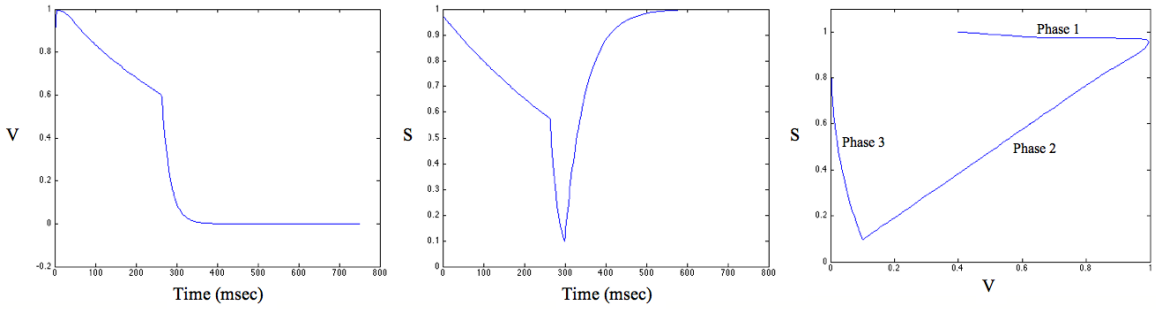

Figure 2: *Two figures on the left are the time plots of voltage (left) and slow gate variable (middle) for a single action potential. On the right is a plot of slow gate vs voltage within the same time frame.*

2.2 Multiple Stimuli and the Restitution Curve

Previously, when a single stimulus was applied, it produced an action potential but afterward the cell moved itself back to the equilibrium state. This time we will feed the cell with a sequence of equally spaced stimuli, and observe its behavior. It turns out that when the gaps between stimuli are wide enough, the result is trivial: i.e. the cell responds to the stimuli with repeated action potentials, all essentially identical to the response to a single stimulus. However, when we feed the cell with stimuli whose pacing is fast enough, the responses, including the action potential durations, could be different from stimulus to stimulus within the same sequence of stimuli. This also leads to different long term behaviors such as alternans and 2:1 (two stimuli produce only one action potential), as discussed below.

The action potential duration (APD) is one of the measures used to distinguish cell responses. Precisely, it is defined to be the time during which the voltage exceeds v_{crit} which includes phase 2 and most of phase 1. The diastolic interval (DI) is defined as the duration between the end of the an action potential and the arrival of the next stimulus, or, in other words, the length of phase 3. This DI will be a proxy of how much the gate variables have recovered. The goal of this section is to study how responses differ, particularly in APDs, when the gates are not fully open upon the arrival of a stimulus. We will derive the function Φ in eq.(4) which describes an approximate relationship between DI and its following APD:

$$\Phi(DI_n) = APD_{n+1} = \tau_{sclose} \ln \left(\frac{(1-(1-v_{crit})e^{\frac{-DI_n}{\tau_{open}}})\delta}{v_{thr}} \right) + \tau_{ung} \ln \left(\frac{v_{thr}}{v_{crit}} \right) + 16, \qquad ------(4)$$

where δ is a discount factor whose formula is given in (7).

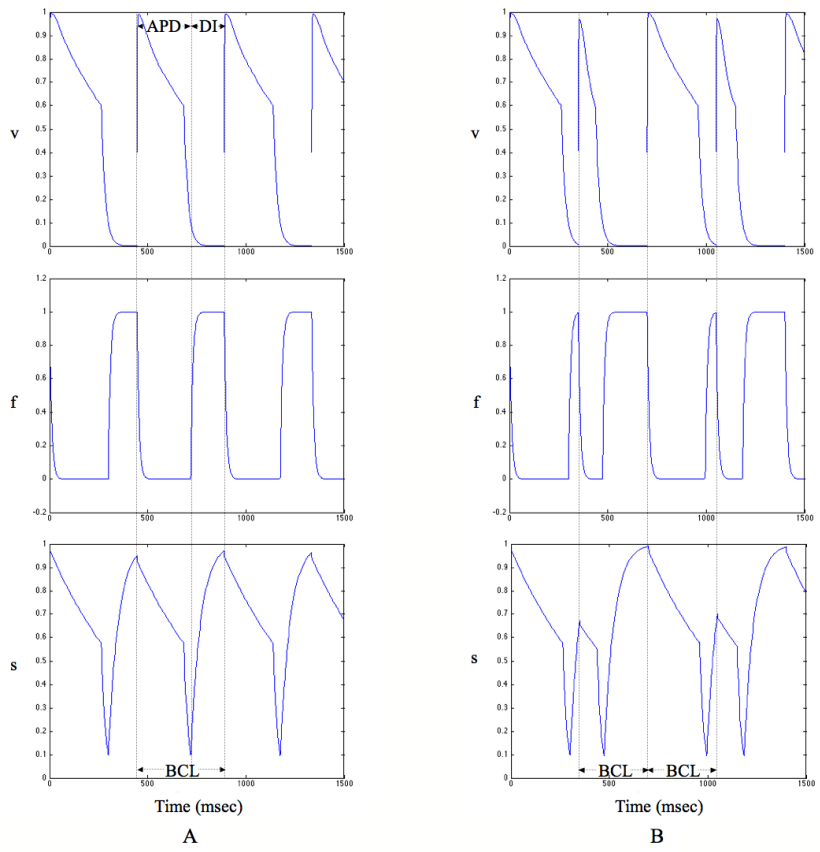

Figure 3: *Graphs of voltage and gate variables over time describing cell responses to multiple stimuli with, on the left, BCL = 445 msec and BCL = 350 msec in B. In A, the response is trivial: APDs are all identical and equal to 274.5 msec, DI = 170.5 msec. In B the cell responds with two alternating APDs, the behavior referred to as alternans.*

- Starting at the beginning of phase 3 prior to the arrival of the considered stimulus, we would like to examine the dependence of gate variables on the DI. We assume, using the approximation that will be derived later, that initially $s = v = v_{crit}$ and $f = 0$. During this phase, the gate variables reopen, trying to move toward the equilibrium $(v, f, s) = (0, 1, 1)$. In fact, f opens very quickly and much faster than s. This fact leads to the assumption that, for a typical DI, f will fully recover before the stimulus arrives. The slow gate, on the other hand, will not fully open. The relationship between DI and the slow gate at the arrival of the stimulus (s_i) derived by explicitly solving (3) is given as
$$s_i = 1 - (1 - v_{crit})e^{-DI/\tau_{open}}. \qquad ------(5)$$

- Next, the cell enters an action potential starting in phase 1, the phase which characterized by a rapid rise in voltage but a small change in slow gate variable. To be more elaborate, phase 1 is divided into two smaller phases by the closing rate of s: phase 1a, when $v_{vstim} < v < v_{thr}$, and phase 1b, when $v > v_{thr}$. During 1a, s closes rapidly by the time scale of τ_{fclose} while f and s approximately equal 1. Despite its smallness, the change in s is significant to the accuracy of the estimation of APD. We will calculate δ, the discount factor of s, which will determine how much s drops over phase 1a. On the contrary, in phase 1b, s decreases rather slowly by the time scale of τ_{strong}. The change in s in this phase is therefore negligible. This is evident in the plot of s and v in figure 2 as the line trajectory describing the movement of (v, s) in phase 1b is flat and almost horizontal. Furthermore, we assume that $v \approx 1$ at the end of phase 1b where it begins to drop. This is true because J_{strong}, which is of

the highest leading order in eq.(1), would continue pushing further the voltage and not wear off until v reaches 1.

Now let's calculate the discount factor δ during phase 1a. We use $f \approx 1$ and neglect the ungated current which is currently dominated by the strong current. The equation underlying the change in v is then written as

$$\frac{dv}{dt} = (1-v)/\tau_{open} \qquad ------(6)$$

As a result of solving (6) subject to the initial and final values of v, the calculated time for phase 1a is $\tau_{strong} \ln((1-v_{stim})/(1-v_{thr}))$ (this is indeed close to zero). Consequently, by solving (3) and substituting the time in phase 1a we obtain

$$\delta = \left(\frac{1-v_{thr}}{1-v_{stim}}\right)^{(\tau_{strong}/\tau_{fclose})}. \qquad ------(7)$$

- Similarly, phase 2 consists of two smaller phases which are 2a: $1 > v > v_{thr}$, and 2b: $v_{thr} > v > v_{crit}$. We will prove the statement mentioned earlier that, in the typical setting, $s \approx v_{crit}$ regardless of what may have happened earlier in phase 2. In the mean time, we will estimate time duration in each phase which will be done by considering the decrement of s and tracing back the time from the differential equation (3).

  - At the beginning of phase 2a, we suppose that the initial values of variables are $v(0) \approx 1$, $s(0) = \delta s_i$ (discounted from the initial value at phase 1), and $f(0) \approx 0$. The slow gate variable as a function of time directly derived from (3) is given by

    $$s(t) = \delta s_i e^{-t/\tau_{close}}. \qquad ------(8)$$

    Eq.(1) after the elimination of J_{strong} and substitution of (8) in s, is reduced to

    $$\frac{\partial v}{\partial t} = \frac{\delta s_i e^{-t/\tau_{sclose}}}{\tau_{weak}} - \frac{v}{\tau_{ung}} \qquad ------(9)$$

    Multiplying (9) by integrating factor and solving, we obtain

    $$v(t) = A_1 e^{-t/\tau_{sclose}} + B_1 e^{-t/\tau_{ung}}, \qquad ------(10)$$

    $$\text{where } A_1 = \frac{\delta s_i/\tau_{weak}}{1/\tau_{ung} - 1/\tau_{sclose}} \approx \delta s_i, \qquad ------(11)$$

    $$\text{and } B_1 \approx 1 - \delta s_i. \qquad ------(12)$$

    Note that the approximation in (11) comes from the assumption $\tau_{weak} \approx \tau_{ung} \ll \tau_{sclose}$. This, however, leads to an estimation error which will be discussed in detail later. At the end of phase 2a, the term $\delta s_i e^{-t/\tau_{sclose}}$ dominates $(1-\delta s_i)e^{-t/\tau_{ung}}$ because the exponent in the first term is negative and much smaller. For this reason, the second term in (10) is ignored, the approximation of the voltage toward the end of the phase is simply

    $$v(t) \approx \delta s_i e^{-t/\tau_{sclose}} = s(t) \qquad ------(13)$$

    Therefore, the estimated value of s at the end of phase 2a is v_{thr}.

  - During phase 2b, both J_{strong} and J_{weak} vanish completely, letting J_{ung} alone drive the system. The underlying differential equation of v is simplified to

    $$\frac{dv}{dt} = \frac{-v}{\tau_{ung}}, \qquad ------(14)$$

    with the boundary condition $v(0) = v_{thr}, s(0) \approx v_{thr}$, and $v_{end} = v_{crit}$. From (14) and the second line of (3), we observe that the starting values and the declining rates of v and s are the same. Hence we conclude that the ending values of v and s should be approximately identical and equal to v_{crit} and consequently prove the first claim. Moreover, solving (14) with boundary condition yields an estimation of the length of phase 2b:

    $$T_{2b} = \tau_{ung} \ln(v_{thr}/v_{crit}). \qquad ------(15)$$

  - Lastly, we would like to estimate the time duration for phases 1b and 2a which together can be done by solving ODE in the first line of (3) with the boundary condition: $s(0) = \delta s_i$ and $v(T_{1b+2a}) = v_{thr}$. Doing so we obtain

    $$T_{1b+2a} = \tau_{sclose} \ln(\delta s_i/v_{thr}) + C, \qquad ------(16)$$

    where C is a correction for the errors made in the approximation (11).

Finally, putting together (5, 15, 16) and estimating $C \approx 16$ msec by fitting the estimated curve (16) with the data from computer simulation, we successfully construct the restitution curve or the function Φ

in eq.(4). As we will see in Figure 5, the prediction is very accurate.

2.3 Alternans and Other Behaviors in the Long Term

The restitution curve in (4) describes a single APD based on the previous DI, but does provide any illustrations of the overall sequence of APDs for serial stimuli. When a heart cell is disturbed by a sequence of stimuli, its responses are actually not arbitrary. At the beginning we might observe a transient, a short-term behavior where APD jumps from one to another apparently randomly, but if we wait longer, we will see that the responses gradually converge to a long-term periodic pattern which can be either alternans, 1:1, 2:1, or others. In this section, we will consider, by simulation and mathematical analysis of the model, such patterns of the heart cell's responses as well as predicting which pattern will occur for a given sequence of stimuli.

Let BCL denote the time space between two consecutive stimuli which is all the same for an equally spaced sequence of stimuli. For the purpose of studying the cell behavior, we would like to construct a plot of BCL and APD. This plot will provide useful information of the cell behavior. For instance, if the cell demonstrates alternans behavior, we would see two points of APDs marked on the same level of BCL. Similarly, if there is only one mark of APD on a value of BCL and $APD < BCL$, we can conclude from the plot that the response pattern is 1:1 behavior.

First, we begin to construct the plot of BCL and APD from simulation. The method used in this simulation is the "decreasing BCL" method whose procedures can be described as follows:

- Step 1: Start from large BCL where the BCL is long enough so that the response pattern is trivial (1:1 and the cell returns to the fully recovered state $(v, f, s) = (0, 1, 1)$ before the arrival of next stimulus).
- Step 2: Compute the numerical solution of differential equations (1,2,3) with external stimuli exerted into the system for time t = nBCL for many integers n. The running time for this step should be long enough that it allows the cell to establish a long-term periodic pattern.
- Step 3: Record all the APDs when the cell enters into such a pattern.
- Step 4: If BCL is still within scope of the study, reduce BCL with a small decrement. Repeat Steps 2, 3, and 4 using the ending values of v, f, and s as the initial values at time t = 0.

Figure 5 shows the plot of BCL and APD from the simulation. For $BCL > 368$ msec, the cell exhibits a stable 1:1 behavior. As BCL decreases below 368 msec, this 1:1 behavior becomes unstable. The heart evolved to what is called *alternans*, a response producing two action potentials alternating between short and long in the stable state. For even shorter BCL ($297 < BCL < 368$ msec), we observed a 2:1 behavior, an event in which only every other stimulus produces an action potential. The behavior of the cell becomes more complicated when BCL is very short, however, it is not in the scope of our study.

We would like also to provide mathematical understanding of the changes in the cell behaviors. Recall that eq.(4) describes a relationship between APD and DI. We can rewrite it in terms of APD and BCL as

$$\Phi(BCL - APD_n) = APD_{n+1} = \tau_{sclose} \ln \left(\frac{(1-(1-v_{crit})e^{\frac{APD_n - BCL}{\tau_{open}}})\delta}{v_{thr}} \right) + \tau_{ung} \ln \left(\frac{v_{thr}}{v_{crit}} \right) + 16, \quad ----(17)$$

where APD_n and APD_{n+1} denote the action potential durations corresponding to current and the next stimuli respectively. Two important properties of function Φ which will be used in the following analysis are its strict monotonicity and concavity; these properties are clearly evidenced in figure or directly verified from eq.(4). To find out what are the APDs, we solve for fixed points (APD^*) in the equation

$$APD^* = \Phi(BCL - APD^*). \quad ------(18)$$

For a large and fixed BCL, $\Phi(BCL - APD)$ as a function of APD is guaranteed to have a unique fixed point. The uniqueness comes from the fact that $\Phi(BCL - APD)$ is strictly decreasing with respect to APD. However, the solution of (18) which indicates 1:1 behavior is not necessarily stable. According to the linear stability of a fixed point given by Strogatz [8], the condition below implies the stability of 1:1 behavior:

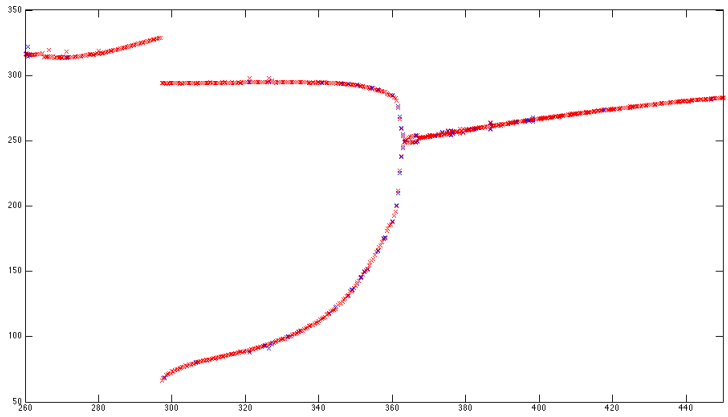

Figure 4: *Graph of BCL (x-axis) vs APD (y-axis) from a computer simulation.*

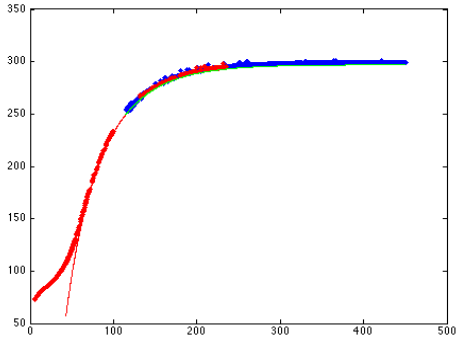

Figure 5: *Graph of APD vs DI obtained by tracing back from Figure 4. The red dots correspond to 1:1 behavior ($BCL > 368$), the blue dots, alternans ($297 < BCL < 368$). The thin line is the estimation function from eq.(4).*

$$|\Phi'(BCL - APD^*)| < 1. \qquad ------(19)$$

We can find the bifurcation point where 1:1 behavior loses stability and becomes alternans by violating eq.(19), i.e. solving for $DI^* = BCL - APD^*$ such that $|\Phi'(DI^*)| = 1$. In fact, we can write Φ' explicitly as

$$\Phi'(DI) = \frac{\tau_{sclose}}{\tau_{open}} \frac{(1-v_{crit})e^{-DI/\tau_{open}}}{1-(1-v_{crit})e^{-DI/\tau_{open}}}. \qquad ------(20)$$

Hence, the formula for DI at bifurcation is

$$DI^* = \tau_{open} \ln(\frac{(\tau_{sclose}+\tau_{open})(1-v_{crit})}{\tau_{open}}). \qquad ------(21)$$

Numerically, $DI^* \approx 115$ msec, $APD^* \approx \Phi(115) = 249$ msec, thus $BCL_{bif} \approx 364$ msec. This result from calculation is quite accurate in comparison to the result from computer simulations.

3 Extension of Model to a Heart Fiber

In this section, we would like to extend the model (1, 2, 3) of a single heart cell to a heart fiber. The new model consists of three partial differential equations, one of which incorporates an additional diffusion term which distinguishes it from the model of a single cell. The formal form of the model is given as

$$\frac{\partial v}{\partial t} = \kappa \frac{\partial^2 v}{\partial x^2} + J_{strong}(v,f) + J_{weak}(v,s) - J_{ung}(v), \quad ------(22)$$

$$\frac{\partial f}{\partial t} = \begin{cases} \frac{-f}{\epsilon_{close}} & \text{, if } v > v_{crit}; \\ \frac{(1-f)}{\epsilon_{open}} & \text{, if } v < v_{crit}, \end{cases} \quad ------(23)$$

$$\frac{\partial s}{\partial t} = \begin{cases} \frac{-s}{\tau_{sclose}} & \text{, if } v_{thr} < v; \\ \frac{-s}{\tau_{fclose}} & \text{, if } v_{crit} < v < v_{thr}; \\ \frac{1-s}{\tau_{open}} & \text{, if } v < v_{crit}, \end{cases} \quad ------(24)$$

where κ denotes a diffusion coefficient which is set up to be 0.001 cm^2/msec.

To demonstrate the dynamics of the model, let's assume that the heart fiber of length L (of length up to 10 cm) is stimulated at the left end near x = 0 (the default stimulated length is 0.5 cm). The stimulation causes a building up of high potential on the left end which will propagate to the right through a diffusion process, the same phenomenon observed in the two-current model by Cain and Schaeffer [5]. Furthermore, when we apply periodic stimuli the output response looks like waves of many layers propagating to the right. Based on this observation, we will seek a traveling wave solution of the system (22, 23, 24) and estimate speed of the wave.

3.1 Traveling Wave Solutions and the Estimation of Wave Speed

First consider a single pulse on an infinitely long heart fiber. Suppose a traveling wave solution of the system of PDEs (22, 23, 24) is

$$v(x,t) = V(t + x/c), \quad f(x,t) = F(t + x/c), \quad s(x,t) = S(t + x/c),$$

where the speed c is to be determined. Let $\xi = t + x/c$, then V, F, and S are functions depend only upon ξ. We'll solve this system approximately in terms of matched asymptotics by solving separately for the wave-front layer ($\xi \approx 0$) and the outer layers ($\xi < 0$ and $\xi > 0$).

In the outer layer $\xi < 0$, the traveling wave solution is trivial: $V \equiv 0, F \equiv S \equiv 1$. The outer layer $\xi > 0$, on the contrary, has a leading-order solution identical to the solution of the ODEs in a patch.

In the wave-front layer, where the time is $O(\tau_{strong})$, we may approximate $F \equiv 1$ and $S \equiv 1$ because the time constants governing changes in F and S are much larger than τ_{strong}. To find the wave-front solution, we use a scaled coordinate $\tilde{\xi} = \tau_{strong}^{-1}(t + x/c)$ and solve the ordinary differential equation

$$V' = \frac{1}{c^2}\frac{\kappa}{\tau_{strong}} V'' + \tau_{strong}\left[J_{strong}(V,1) + J_{weak}(V,1) - J_{ung}(V)\right]$$

where prime indicates differentiation with respect to the scaled variable $\tilde{\xi}$. The weak and ungated currents are negligible since $\frac{\tau_{strong}}{\tau_{weak}} \ll 1$, $\frac{\tau_{strong}}{\tau_{ung}} \ll 1$. We solve for the approximate solution by dividing the wave-front layer itself into two layers according to breakdown of the strong current:

1. $\tilde{\xi} < 0$ and $V < v_{crit}$. In this layer, the strong current is identically zero and does not contribute any voltage to the account. Thus, the solution is underlined by simple equation

$$V' = \frac{1}{c^2}\frac{\kappa}{\tau_{strong}} V'', \text{ for } \tilde{\xi} < 0$$
$$\text{subject to: } \lim_{\tilde{\xi}\to -\infty} V(\tilde{\xi}) = 0 \text{ and } \lim_{\tilde{\xi}\to 0^-} V(\tilde{\xi}) = v_{crit}. \quad -----(25)$$

2. $\tilde{\xi} > 0$. In this layer is different from the previous in that $v_{crit} < V < 1$, and so $J_{strong} = 1 - V$. The equation to solve is

$$V' = \frac{1}{c^2}\frac{\kappa}{\tau_{strong}} V'' + (1 - V), \text{ for } \tilde{\xi} > 0$$
$$\text{subject to: } \lim_{\tilde{\xi}\to 0^+} V(\tilde{\xi}) = v_{crit} \text{ and } \lim_{\tilde{\xi}\to +\infty} V(\tilde{\xi}) = 1. \quad -----(26)$$

The two layers meet where $\tilde{\xi} = 0$ at the value $V(0) = v_{crit}$. Both ODEs (25) and (26) are linear of second order, hence solvable and the result is:

$$V(\tilde{\xi}) = \begin{cases} v_{crit} e^{\tilde{\xi}/\alpha}, & \text{for } \tilde{\xi} < 0 \\ (v_{crit} - 1)e^{\lambda_- \tilde{\xi}} + 1, & \text{for } \tilde{\xi} > 0 \end{cases}$$

where $\alpha = \frac{1}{c^2}\frac{\kappa}{\tau_{strong}}$ and $\lambda_- = \frac{1-\sqrt{1+4\alpha}}{2\alpha}$. Moreover, we want the solution to be smooth everywhere including at the connecting point $(\tilde{\xi}, V) = (0, v_{crit})$. In particular, the speed c will be determined so that

$$\lim_{\tilde{\xi}\to 0^-} V' = \lim_{\tilde{\xi}\to 0^+} V'.$$

As a result from solving the above equation, $\alpha = ((\frac{1+v_{crit}}{1-v_{crit}})^2 - 1)/4 \approx 0.1235$, which yields an estimation c:

$$c = 2.846\sqrt{\frac{\kappa}{\tau_{strong}}} \approx 9 \times 10^{-2} \text{ cm/msec.} \qquad ------(27)$$

Above, we have calculated the traveling wave speed when $f = s = 1$ upon the arrival of a stimulus, however, the wave speed is different when the gates are not fully open. In fact, it turns out that the wave speed depends mostly on the fast gate variable. The derivation of c as a function of f below comes from the same calculation as the earlier finding of wave-front solutions but using a new scaled variable $\tilde{\xi} = \frac{f}{\tau_{strong}}(t + x/c)$:

$$c(f) = 2.846\sqrt{\frac{\kappa f}{\tau_{strong}}}. \qquad ------(28)$$

In turn, the fast gate upon the arrival of a stimulus is determined by DI which is given by

$$f(DI) = 1 - e^{-DI/\epsilon_{open}}. \qquad ------(29)$$

Together, eq.(28, 29) leads to a formula estimating the traveling-wave speed as a function of DI,

$$c(DI) = 2.846\sqrt{\frac{\kappa(1-e^{-DI/\epsilon_{open}})}{\tau_{strong}}}. \qquad ------(30)$$

3.2 Discordant Alternans

The case discussed above–that the output response to a periodic stimulation is a periodic traveling wave– is valid for long BCL when 1:1 behavior occurs throughout the heart fiber. When alternans occur, however, the traveling wave suffers phase reversals whose effect may vary at different locations, a phenomenon known as discordant alternans. Dai and Schaeffer predict two different types of discordant alternans, distinguished by the characteristics of phase reversals which can be either stationary or moving [6]. Their study shows that, unless using a complicated model, the two-current model exhibits traveling discordant alternans, in which the amplitude of the phase reversals is always changing. We will investigate the three-current model in a similar way. First, we will simulate, on a heart fiber with finite length, $APD(x)$ corresponding to several beats of stimuli. Then we will attempt to provide mathematical evidence using the theory borrowed from Dai and Schaeffer [1].

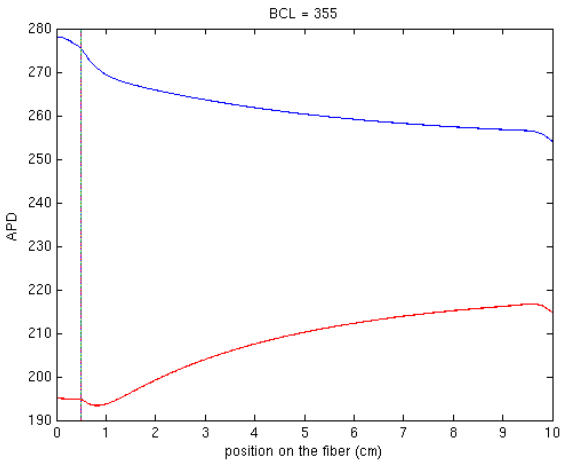

Figure 6: *Plot of APD along the cardiac fiber. The top (blue) line represents APDs corresponding to even pulses, and the bottom (red), the odd pulses.*

The result from computer simulations in figure 6 shows that discordant alternans occurring in the three-current model (with the given values of parameters) is stationary. Once the simulation enters the stable state, the phase reversals, though alternating between short and long, repeat the exact same pattern throughout rest of the simulation time. Figure 6 illustrates this phenomenon; the responses are identical for every other pulse as the line indicating APDs corresponding to the fifth pulse overlaps with the first and the third. This result is clearly distinguished from the traveling case, in which the phase reversals are always changing causing the heart to never enter a repeating pattern.

Let us show that the theory of Dai and Schaeffer makes the prediction that the discordant alternans is indeed stationary for this model. Their theory requires the computation of parameter $\bar{\Lambda}^{-1}$ defined as

$$\bar{\Lambda} = \Lambda\omega^3\xi^{-4},$$
$$\text{where } \Lambda = \frac{c(DI_{crit})^2}{2\frac{dc}{dDI}|_{DI=DI_{crit}}}, \qquad \omega = \frac{2\kappa}{c(DI_{crit})}, \qquad \xi = \sqrt{\kappa APD_{crit}},$$

and DI_{crit}, APD_{crit} denote the DI, APD at bifurcation respectively. Dai and Schaeffer predict that the discordant alternans is stationary if $\bar{\Lambda}^{-1} \lesssim 2.8$, and it is traveling otherwise. The following table presents numerical values of the variables used in the computation of $\bar{\Lambda}^{-1}$:

	DI_{crit}	APD_{crit}	$f'(DI_{crit})$	$\frac{dc}{dDI}\|_{DI=DI_{crit}}$	Λ	ω	ξ	$\bar{\Lambda}^{-1}$
Numerical	115	249	1.013×10^{-6}	4.558×10^{-8}	8.884×10^{4}	.02222	.4990	.06362

Thus the theory of Dai and Schaeffer predicts that the discordant alternans occurring in this model will be stationary, as is indeed observed. In an expression involving the parameters,

$$\bar{\Lambda}^{-1} \sim \frac{\tau_{sclose}^2(\ln(v_{thr}))^2}{22.768*\tau_{strong}}\left(\frac{\tau_{open}}{\tau_{sclose}(1-v_{crit})}\right)^{\frac{\tau_{open}}{\epsilon_{open}}}.$$

4 Conclusion

We have studied the three-current model of electrical activity of a heart membrane in zero dimension and extended the model to one dimension. In zero dimensions, or the single-cell model, we derived the restitution curve as well as predicting the bifurcation point where alternans occurs as the 1:1 behavior loses its stability. In the one dimensional model, we estimated the traveling wave speed and found that discordant alternans are stationary, which is the main goal of this research paper. We are able to provide simulations along with

the numerical computation of Λ^{-1} to support the result. This finding offers an alternative way to observe stationary discordant alternans, not requiring a physiologically complex model.

The three-current model still needs further study, especially as regards how its behavior changes as parameters are varied. In particular, one wonders whether, as in the two-current model, traveling discordant alternans may occur. This can potentially be achieved by decreasing the ratio of $\frac{\tau_{open}}{\epsilon_{open}}$ and increasing τ_{sclose}. Unfortunately the time was insufficient to permit such computation.

5 Acknowledgments

I am heartily thankful to my research supervisor, David Schaeffer, whose encouragement, guidance and support enabled me to develop an understanding of the subject. Without his guidance and persistent help this project would not have been possible. I would like to thank Matt Bowen, a graduate student at Duke, for his generous advice in C++ programming and sharing his codes for simulations. The simulations for the heart fiber would not have succeeded without his contribution to the project. I would also like to extend my gratitude to Professor Kraines who always provided me good academic recommendations and supported me in every way. In addition, I thank the PRUV program for the research opportunity including the financial support for summer research during my sophomore year. Lastly, I offer my regards and blessings to all of those who supported me in any respect during the completion of the project.

6 References

1. S. Dai and D. Schaeffer, *Bifurcations in a modulation equation for alternans in a cardiac fiber*, ESAIM Mathematical modelling and numerical analysis **44** (2010).

2. B. Echebarria and A. Karma, *Amplitude-equation approach to spatiotemporal dynamicsof cardiac alternans*, Phys. Rev. E **76** (2007).

3. F. Fenton and A. Karma, *Vortex dynamics in three-dimensional continuous myocardium with fiber rotation: filament instability and fibrillation*, Chaos **8** (1998), p20.

4. C. Mitchell and D. Schaeffer, *A two-current model for the dynamics of cardiac membrane*, Bull. Math. Bio **65** (2003), p767–793.

5. J. Cain and D. Schaeffer, *Shortening of cardiac action potential duration near an insulating boundary*, Math. Med. Biol **25** (2008), p21–36.

6. S. Dai and D. Schaeffer, *Spectrum of a linearized amplitude equation for alternans in a cardiac fiber*, SIAM J. Appl. Math **69** (2008), p704–719.

7. E. Tolkacheva, D. Schaeffer, D. Gauthier, and C. Mitchell, *Analysis of the Fenton-Karma model through an approximation by a one-dimensional map*, Chaos **12** (2002), p1034–1042.

8. S. Strogatz, *Nonlinear dynamics and chaos: with applications to physics, biology, chemistry, and engineering*, Westview Press (2001).